Figure S1

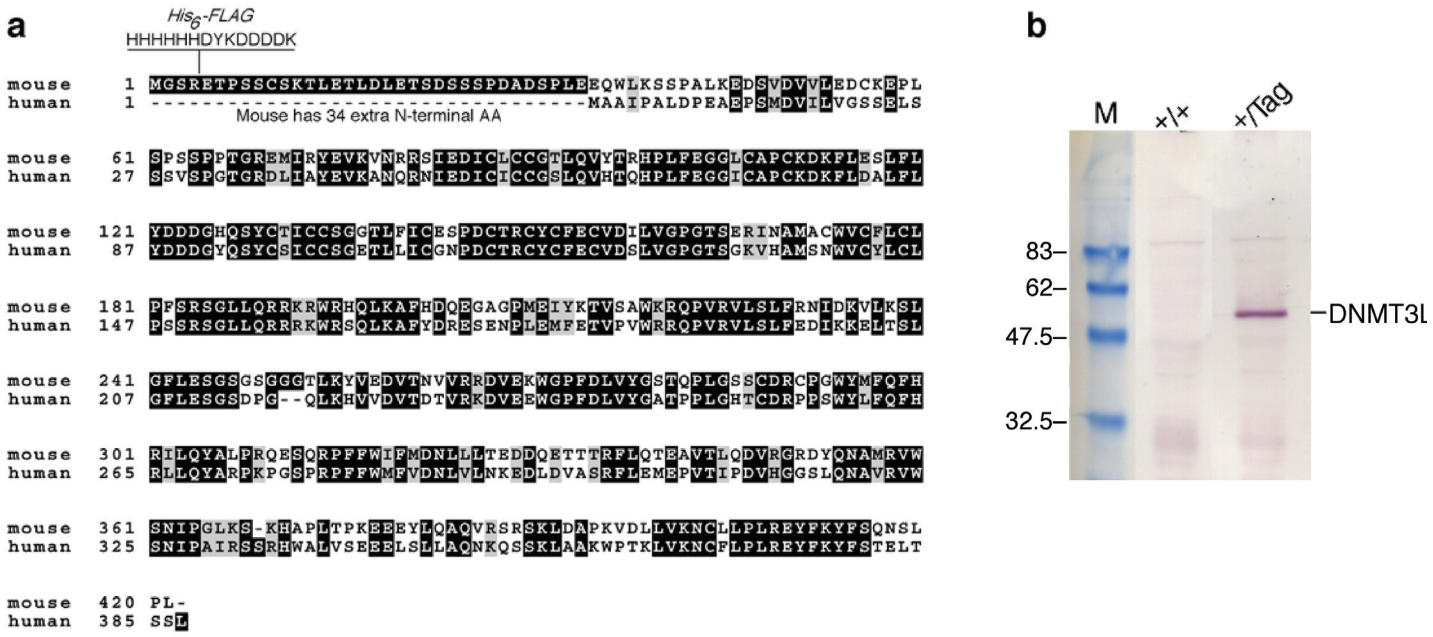

Figure S1: N-terminal epitope tag introduced into the endogenous *Dnmt3L* locus. **a,** Position of epitope tag in DNMT3L. The His_6-Flag tag was added after the first 4 amino acids of DNMT3L. Mouse DNMT3L has a long N-terminal extension not present in human DNMT3L. Introduction of the epitope tags did not cause a discernible phenotype in mice of either sex, while mice homozygous for the null allele are maternal effect lethals in females and cause azoospermia in males. These data indicate that introduction of the epitope tags did not significantly affect the biological activities of DNMT3L. **b**, Detection of epitope tagged DNMT3L by western blot with anti-FLAG antibody in lysates of heterozygous ES cells.

Figure S2

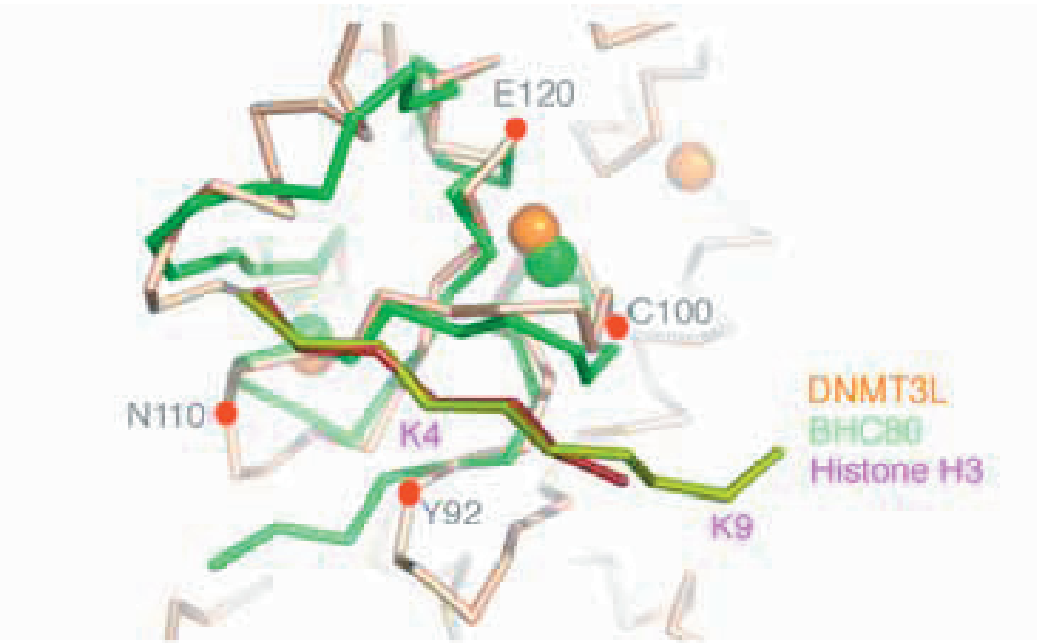

Figure S2: Structural similarity of H3 binding sites on DNMT3L and BHC80. Fan et al. showed methylation-sensitive binding of BHC80 (a component of the LSD1 H3 lysine 4 demethylase complex). The H3 tail binding site has a very similar structure in BHC80 and DNMT3L, with rootmean- square deviation of approximately 0.7 Å comparing the seven pairs of Cα atoms of two bound peptides and 30 pairs of Cα atoms of two proteins (between Y92 and V122 of DNMT3L).

Table S1: Data collection, phasing and refinement statistics for MAD (Zinc) structures of DNMT3L

	Crystal 1 (three-wavelength) (Different part of the crystal used for each wavelength)			Crystal 2 (Zn anomalous)	Crystal 3 (Native 1)	Crystal 4 (peptide soaking)
Data collection						
Space group			$P6_122$			
Cell dimensions						
a=b, *c* (Å)	267.7, 151.1	269.3, 151.8	267.0, 150.9	266.6, 149.5	267.2, 149.5	267.7, 150.0
α, β, γ (°)			90, 90, 120			
	Peak	*Inflection*	*Remote*			
Wavelength (Å)	1.2826	1.2830	1.2199	1.2815	1.0	1.0
Resolution (Å) *	50-4.14 (4.29-4.14)	50-4.66 (4.83-4.66)	50-4.00 (4.14-4.00)	35-3.59 (3.72-3.59)	35-3.29 (3.41-3.29)	35-3.69 (3.83-3.69)
R_{sym} or R_{merge} *	0.092 (0.323)	0.094 (0.426)	0.086 (0.322)	0.078 (0.462)	0.095 (0.489)	0.105 (0.496)
$I/\sigma I$ *	15.0 (8.4)	11.6 (5.7)	17.1 (7.9)	12.8 (3.8)	13.4 (3.9)	11.6 (2.8)
Completeness (%)*	99.8 (100)	99.9 (100)	99.3 (100)	99.1 (100)	98.9 (99.1)	89.4 (89.4)
Redundancy	9.6	9.3	9.4	5.5	5.8	8.0
Refinement						
Resolution (Å)					3.29	3.69
No. reflections					46,954	30,239
R_{work}/ R_{free}					0.248/0.272	0.264/0.302
No. of atoms						
Protein					7,855	8,517
Zinc ion					9	9
B-factors (Å^2)						
Protein					114.0	136.4
R.m.s deviations						
Bond lengths (Å)					0.008	0.008
Bond angles (°)					1.5	1.4

*Highest resolution shell is shown in parenthesis.

The full-length human DNMT3L cDNA (IMAGE clone 3138514) was subcloned into a modified pET-28a (Novagen) vector, which adds a short N-terminal MGHHHHHH tag (pXC391), and expressed in *E. coli.* DNMT3L protein was purified by a nickelchelating column, a HiTrap heparin column and a HiPrep Sephacryl-S300 column (Amersham Biosciences). DNMT3L contains three intrinsic zinc atoms, as determined on a Thermo Jarrell-Ash Enviro 36 ICAP analyzer. The protein was concentrated to 10-15 mg/ml.

Three-wavelength Zn multiple anomalous diffraction (MAD) data (from crystal #1 with size of 0.6_0.3_0.3 mm grown under the conditions of 0.4-0.6 M sodium citrate, 0.1 M bicine, pH 9.0, at 16°C) were collected at the IMCA-CAT beamline at Argonne National Laboratory APS. The data were processed with HKL 2000[1]. Zinc ions were found by SnB[2] at a resolution of 4.5 Å and SOLVE[3] was used to refine the zinc positions, resulting in a figure of merit of 0.53 and the overall Z-score of 25. RESOLVE[4] was applied for density modification and phase extension to 3.59 Å (from crystal #2).

The overall boundaries of the molecule were clearly visible with two domains for each of the three DNMT3L monomers per asymmetric unit: the initial model was built by placement of the structures of human DNMT2 (PDB 1G55) and the KAP-1 PHD domain (PDB 1FP0) into the densities corresponding to the C-terminal and N-terminal domain, respectively, and replacement of amino acids based on sequence alignment between DNMT2 and DNMT3L in the methyltransferase fold, and KAP-1 PHD and DNMT3L in the zinc-binding domain. Initial values of R-factor and R-free were 56.4% and 54.2% at the 3.6 Å resolution. Manual model building using program O[5] was reiterated followed by rigid-body refinement using CNS6 - treating the zinc-binding domain and the methyltransferase domain as two rigid groups with strict non-crystallographic symmetry (NCS) averaging, 80% bulk solvent correction, and a weight with phase restraint to experimental phases. The electron density was calculated with combined experimental and calculated phases. Individual loops were deleted and rebuilt based on omit electron density map. Because of limited resolution (3.6 Å) and an approximately equal number of atomic parameters (8367 atoms x 4 = 33,468) over the number of unique reflections (36,688), we imposed a strict NCS restraint throughout the refinement. To further reduce the number of free parameters to fit the diffraction data, we used group instead of individual Bfactors. Later, higher resolution data at 3.29 Å resolution (from crystal #3 with size of 0.8 x 0.4 x 0.4 mm grown under the conditions of 12% polyethylene glycol 3350 and 0.2 M sodium citrate pH 7.5), measured at the SERCAT-ID beamline of APS, were used for final refinement. Because of an increased number of unique reflections (47,346) at the higher resolution, the NCS was released in the final cycles of refinement, to allow different side chain rotomers and to replace side chains lacking densities with alanines.

Peptide soaked into a pre-formed DNMT3L crystal revealed electron density for the peptide bound in the corresponding position as observed in the BHC80 PHD domain. Omit electron density contoured at 4σ above the mean covers the first residues, while the density contoured at 2σ covers 9-10 residues. The density map was calculated from a 3.69Å resolution data collected from a crystal soaked with H3 peptide (residues 1-24) for 2-3 days.

1. Otwinowski, Z. and Minor, W. (1997) Processing of X-ray Diffraction Data Collected in Oscillation Mode. *Methods in Enzymology*, **276**, 307-326.
2. Weeks, C.M. & Miller, R. (1999). The design and implementation of SnB v2.0, *J. Appl. Cryst.* **32**, 120-124.
3. Terwilliger, T. C. and Berendzen, J. (1999) Automated MAD and MIR structure solution. *Acta Crystallogr* **D55**, 849-861.
4. Terwilliger, T. C. (2000) Maximum likelihood density modification. *Acta Crystallogr.* **D56**, 965-972
5. Jones, T. A., Zou, J. Y., Cowan, S. W. & Kjeldgaard, M. (1991) Improved methods for building protein models in electron density maps and the location of errors in these models. *Acta Crystallogr* **A47**, 110-119.
6. Brunger, A. T. et al. (1998) Crystallography & NMR system: A new software suite for macromolecular structure determination. *Acta Crystallogr* **D54,** 905-21.